ORIGINAL RESEARCH

Quality by Design Approach for Preparation of Zolmitriptan/Chitosan Nanostructured Lipid Carrier Particles – Formulation and Pharmacodynamic Assessment

Randa Hanie Awadeen [ID]
Mariza Fouad Boughdady [ID]
Mahasen Mohamed Meshali [ID]

Department of Pharmaceutics, Faculty of
Pharmacy, Mansoura University,
Mansoura 35516, Egypt

Purpose: Zolmitriptan (ZT) is a selective serotonin agonist that is used for the treatment of migraine. It belongs to BCS class III with high solubility and low permeability. Besides, the drug is subjected to pre-systemic metabolism. Accordingly, new Zolmitriptan/chitosan nanostructured lipid carriers (ZT/CT NLCs) coated with Tween 80 (stealthy layer) have been developed to overcome such demerits.

Methods: The NLCs were developed by combining ultrasonication and double emulsion (w/o/w) techniques. The lipids were Gelucire and Labrasol. Herein, the quality by design (2^3 full factorial design) was scrupulously followed, where critical process parameters and critical quality attributes were predefined. The optimized formulation (F8) was fully characterized with respect to entrapment efficiency (%EE), percentage yield (% yield), particle size, size distribution (PDI), zeta potential (ZP), morphological appearance (TEM). In vitro release, stability study and pharmacodynamic evaluations were also assessed. The optimized freeze dried formula was dispensed in in situ gelling hard gelatin capsule encompassing pectin and guar gum for further in vitro and pharmacodynamic evaluations.

Results: The optimized spherical nanoparticles experienced high percentage EE and yield (78.14% and 60.19%, respectively), low particle size and PDI (343.87 nm and 0.209, respectively), as well as high negative ZP (−25.5 mV). It showed good physical stability at refrigerated conditions. The NLCs dispensed in in situ gelling hard gelatin capsule comprising pectin and guar gum experienced sustained release for 30 h and significantly maintained the pharmacological effect in mice up to 8 h (p < 0.001).

Conclusion: ZT, a BCS class III drug that suffers from poor permeability and pre-systemic metabolism, was successfully maneuvered as nanostructured lipid carrier particles (NLCs). The incorporation of the NLCs in in situ gelling hard gelatin capsules fulfilled a dual function in increasing permeability, as well as sustaining the pharmacodynamic effect. This result would open new vistas in improving the efficacy of other class III drugs.

Keywords: zolmitriptan, factorial design, nanostructured lipid carrier, in situ gelling, pharmacodynamics

Introduction

The oral route of drug delivery has always prevailed over other routes. This may be due to its copious merits like ease of administration, patient compliance as well as cost-effective production techniques.[1] Zolmitriptan (ZT) is a second generation triptan derivative which is used for the treatment of migraine attacks

Correspondence: Randa Hanie Awadeen
Department of Pharmaceutics, Faculty of
Pharmacy, Mansoura University, Mansoura
35516, Egypt
Tel +201002074761
Email Randahany@mans.edu.eg

with or without aura and cluster headaches.[2] According to BCS, it is a class III drug that is characterized by high solubility and low permeability. It has a pKa value of 9.52.[3] The elimination half-life of ZT is 2.5–3 h and its absolute oral bioavailability is about 40% due to hepatic first pass metabolism, thus incurring the current surge for its delivery through the lymphatic system.[4] Zolmitriptan has been formulated as oral dosage forms such as sublingual and orodispersible tablets, soluble and mucoadhesive films.[5] Nasal spray and transfersomes have also been attempted.[6] However, no nanostructured lipid carriers (NLCs) have been maneuvered for ZT.

Lipid-based nanoparticle (LBNP) systems represent one of the most promising colloidal carriers for bioactive agents. They have unique characteristics that make them promising candidates for lymphatic delivery. Lipid nanovesicles have been widely applied for oral and transdermal delivery.[7–9] Among lipid based drug delivery systems, NLCs (second-generation lipid nanoparticles) are attracting attention as alternative colloidal drug carriers.[10] They are considered as a hybrid of spatially solid and liquid lipids that make more imperfections in the matrix, thus allowing more accommodation of drug molecules than solid lipid nanoparticles (SLNs).

The main ingredients of NLCs are solid lipids, liquid lipids, surfactant and water. Labrasol and Gelucire which have HLB value of about 13–14 are reported for their ability to improve oral bioavailability.[11] Labrasol (Caprylocaproyl macrogol-8 glycerides) is mainly composed of PEG esters with medium chain glycerides.[12] Gelucire 50/13 (Stearoyl macrogol-32 glycerides) consists of well-characterized PEG-esters, a small glyceride fraction and free PEG.[13] Tween 80 is a water-soluble nonionic synthetic surfactant with HLB value of 15 and is therefore suitable for stabilization of NLC.[14]

Chitosan (CT) is a linear cationic polysaccharide that consists of arbitrarily distributed β-(1–4)-linked d-glucosamine and N-acetyl-d-glucosamine.[15] It has a pKa value of 6.5. It is insoluble at high pH but dissolves at a low one.[16] It has distinctive mucoadhesion with absorption enhancing characteristics and other favorable biological properties like biodegradability, biocompatibility, low immunogenicity and absence of toxicity.[17] It also possesses powerful in-situ gelling properties through pH-dependent hydration mechanism[18] and ionic crosslinking with anionic polymers.[19]

Pectin and guar gum from plant origin are known as viscosity improving agents. They are approved by the US

Food and Drug Administration (FDA) and are officially stated in the United States Pharmacopoeia (USP).[20,21]

The aim of this research is to overcome the poor permeability of ZT through preparation of NLCs containing CT. Double emulsion w/o/w technique with CT solution containing ZT as the internal phase will be followed. The optimized NLCs would be coated with a stealth layer of Tween 80 to enhance permeability. To sustain the pharmacodynamic effect, the NLCs will be dispensed in in situ gelling polymers of plant origin (Pectin and Guar gum) in a hard gelatin capsule.

Materials and Methods
Materials

Zolmitriptan (ZT) Batch # ZT0010615 was kindly supplied by Amoun Pharma Co. (Egypt). Gelucire 50/13 pellets and Labrasol were kindly supplied by Gattefossé (Saint-Priest Cedex, France). Low molecular weight chitosan (CT) (molecular weight = 161.16, degree of deacetylation 93%) was obtained from Oxford Chem. Lab. (India). Guar gum, was obtained from Sigma-Aldrich Co. (St. Louis, MO., USA). Pectin, Batch No. Sonwu 150,310 was obtained from Xi'an Sonwu Biotech Co., Ltd. (China). Tween 80 was obtained from El Gomhoria Co. (Cairo, Egypt). Hard gelatin capsules of size 0 were purchased from CapsuICN International Co., Ltd. (USA). Acetic acid was purchased from EL-Nasr pharmaceutical chemicals Co. (Cairo, Egypt).

Application of Full Factorial Design for Optimization of NLCs

A design of experiment (DOE) (2^3 full factorial design) has been used in order to look into the key effects, as well as interactions of three critical process parameters (CPPs), namely, solid lipid (Gelucire) amount (A), liquid lipid (Labrasol) volume (B) and concentration of CT solution (C), on the prepared NLC critical quality attributes (CQAs), namely, % EE (R1), % yield (R2), particle size (R3) and polydispersity index (R4). This statistical design is very precise and accurate to unveil the main effects and interaction between the CPPs on the formulation CQAs and to study the robustness of the process. The three CPPs were set at high and low levels on the basis of the preliminary study. The coded values of different variables are shown in Table 1. Eight NLC formulations, each with three runs, were prepared in accordance with the design and characterized for the aforementioned CQAs. The

Table 1 CPPs Levels, CQAs and Their Constraints of 2^3 Full Factorial Design

CPPs	Minimum Level	Maximum Level	Minimum Coded Level	Maximum Coded Level
A: Gelucire amount (mg)	150	300	−1	+1
B: Labrasol volume (mL)	0.15	0.3	−1	+1
C: Chitosan solution concentration (% w/v)	0.3	1	−1	+1

Notes: The volume of the internal aqueous phase was kept to half of the oil phase. The amount of drug was kept constant at 5 mg.

model was assessed regarding statistical significance through analysis of variance (ANOVA) using Design-Expert software (Design-Expert 11, State-Ease Inc., Minneapolis, USA) (Table 2).

The complete first order polynomial regression equation was produced as follows:

$$Y = \beta_0 + \beta_1 A + \beta_2 B + \beta_3 C + \beta_4 AB + \beta_5 AC + \beta_6 BC + \beta_7 ABC$$

Where:

Y is the CQAs;

A, B and C are the CPPs;

β_0 represents the arithmetic mean response of the eight runs;

β_1, β_2 and β_3 correspond to the linear coefficients;

β_4, β_5 and β_6 correspond to the coefficients of interaction between the two CPPs; and

β_7 corresponds to the coefficients of interaction between the three CPPs.

Preparation of ZT-Loaded NLCs

ZT-loaded NLCs were prepared through combining ultrasonication and double emulsion (w/o/w) techniques. Accordingly, accurately weighed quantities of Gelucire (150 or 300 mg) and Labrasol (0.15 or 0.3 mL) were heated at 10–15°C above the melting point of Gelucire (50°C) to form a clear uniform oil phase. The internal aqueous phase was composed of a constant amount of ZT (5 mg) that was dissolved either in 0.3 or 1% w/v CT solution (in 1% v/v aqueous acetic acid). The volume of the internal aqueous phase was kept to be half that of the oil phase. Subsequently, the aqueous phase was added to the previously melted oil phase at the same temperature. The melt containing the drug was rapidly solidified with size reduction in a dry ice bath using ultrasonic homogenizer (Cole-Parmer Instrument Co., Chicago, IL, USA) for 3 minutes (90% amplitude) to form a primary w/o emulsion. After that, aqueous surfactant dispersion took place by adding 30 mL of cold deionized water containing 0.1% Tween 80 under ultrasonic homogenization in ice bath for 10 min to produce a double emulsion (w/o/w). The obtained formula was stirred on a magnetic stirrer (Heidolph, USA) for 30 min at room temperature. The NLCs were isolated by centrifugation (11,000 rpm) for 90 min (Sigma, D-37,520, Germany) and then subjected to freeze drying under vacuum (SIM-FD8-8T, USA) at −80°C to obtain the final lyophilized product that was stored at 5°C for further evaluation.

Characterization and Optimization of ZT-Loaded NLCs
Entrapment Efficiency Percent (% EE)

% EE of ZT-loaded NLCs was indirectly determined after centrifugation through measurement of the amount of un-entrapped ZT in the clear supernatant.[22] The prepared

Table 2 Formulations and CQAs Values of ZT-Loaded NLCs Prepared According to 2^3 Full Factorial Design (See Table 1 for Composition)

Formula Code	Code of (A, B, C)	* % Entrapment Efficiency (% EE)	* % Yield	*Particle Size (nm)	* PDI
F1	(+, +, −)	42.22 ± 0.342	25.74 ± 0.01	395.43 ± 13.69	0.136 ± 0.03
F2	(+, −, −)	47.79 ± 0.208	23.95 ± 0.005	214.60 ± 3.045	0.206 ± 0.004
F3	(−, +, −)	48.48 ± 0.204	24.31 ± 0.008	217.97 ± 0.569	0.255 ± 0.021
F4	(−, −, −)	69.84 ± 0.416	44.54 ± 0.006	209.33 ± 2.136	0.127 ± 0.015
F5	(+, +, +)	47.45 ± 0.278	50.11 ± 0.004	666.93 ± 4.366	0.172 ± 0.023
F6	(+, −, +)	61.12 ± 0.267	48.29 ± 0.006	362.87 ± 6.503	0.257 ± 0.016
F7	(−, +, +)	54.46 ± 0.208	49.59 ± 0.001	370.97 ± 2.601	0.239 ± 0.004
F8	(−, −, +)	78.14 ± 0.208	60.19 ± 0.001	343.87 ± 19.704	0.209 ± 0.007

Note: *Mean of three determinations ± S.D.

NLCs were centrifuged at 11,000 rpm for 90 min. The obtained supernatant was filtered through 0.45 Millipore filter (Bedford, MA, USA) of pore size 0.45 μm (Berlin, Germany) and the absorbance of this clear supernatant was measured spectrophotometrically (Ultraviolet-Visible spectrophotometer (Shimadzu, UV-150-02, Sersakusho, Ltd, Kyoto, Japan)) at the predetermined λ_{max} (282 nm) after suitable dilution with 0.1 N HCl of pH 1.2 similar to the standard curve. Plain NLCs were similarly treated and the obtained supernatant was used as a blank. The % EE was determined using equation 1:

$$\%EE = \frac{Amount\ of\ entrapped\ drug}{Total\ amount\ of\ drug}\ x\ 100 \qquad (1)$$

Where:

Amount of entrapped drug = Total drug amount – unentrapped drug amount

Percentage Yield (% Yield)

The percent yield for each formula was calculated as the total weight of dry nanoparticles prepared in relation to the summation of weights of starting materials (drug, lipids and polymers) using equation 2:

$$\%\ yield = \frac{W_m}{W_t}\ x100 \qquad (2)$$

Where, W_m is the actual weight for the prepared lyophilized NLCs,

W_t represents summation of weights of starting materials.[23]

Particle Size and Particle Size Distribution (PDI)

The average particle size and PDI of the freshly prepared NLC formulations were determined using photon correlation spectroscopy particle size analyzer (Zetasizer, ZEN 3600, Malvern, UK). The analysis was performed after proper dilution with deionized water.[24]

Evaluation of the Optimized ZT-Loaded NLC Formula (F8)

Zeta Potential (ZP) Determination

Zeta potential is one of the important parameters for the characterization of the NLC system stability. It measures the surface charge of the particle based on their electrophoretic mobility. ZP of the selected freshly prepared NLCs was measured using photon correlation spectroscopy instrument (Zetasizer) at 25°C. The formula was suitably diluted with deionized water before measurement and the surface charge on the NLCs was specified by

detecting their electrophoretic mobility in an electrical field. Results were obtained as mean values (n=3 ± SD).[25]

Transmission Electron Microscope (TEM)

The morphological examination of the freshly prepared NLCs (F8) was performed using TEM. One mL of the freshly prepared NLC suspension was subjected to tenfold dilution using deionized water, then sonicated for 5 min via ultrasonic bath (Sonix USA, SS101H230). Subsequently, one drop of the diluted suspension was placed on the surface of carbon-coated copper grids (200 mesh, Science Services, Munich, Germany). The excess material was removed with a filter paper leaving a thin film stretched over the holes. The sample was left to dry at room temperature for 10 min. before examination.[26] Capture and analysis of the image were carried out by digital micrograph together with soft imaging viewer software.

Fourier Transform Infrared Spectroscopy (FTIR)

FTIR spectra of: ZT, Gelucire, CT, physical mixtures corresponding to the optimized formula and drug-loaded NLC (F8) were taken via Mattson 5000 FTIR Spectrophotometer (Madison Instruments, Middleton, WI, USA). The wave number region of scanning was over a range of 500 to 3900 cm^{-1}.

Differential Scanning Colorimetry (DSC)

DSC was performed using Perkin-Elmer Differential scanning colorimeter (DSC Perkin Elmer DSC 7, USA, with data analysis system) which was calibrated with indium (99.99% purity, m.p. 156.6°C) at heating rate of 10°C/min. One to five milligrams of each of ZT, Gelucire, CT, physical mixtures corresponding to the optimized formula and drug-loaded NLC (F8) were heated in aluminum crimped pans under nitrogen gas flow (30 mL/min), in the range of 30–450°C. An empty pan sealed in the same way was used as a reference.

Stability Study of the Optimized Formula (F8)

Stability study was carried out as stated in the ICH guidelines. Freshly prepared ZT-loaded NLC aqueous dispersions of (F8) were packed in glass bottles and maintained at ambient conditions (25 ± 2 °C/40% RH ± 5%), as well as at refrigerated temperature (5 ± 3 °C) without any agitation or stirring for 3 months.[23] The stability of the optimized formula was evaluated with respect to physical appearance, percentage drug retention, ZP, particle size

and PDI. The measurements were carried out initially and after storage for 1, 2 and 3 months.

Formulation of the Optimized ZT-NLCs (F8) in in situ Gelling Hard Gelatin Capsule
Choice of the in situ Gelling Polymers

Pectin and guar gum were chosen as in situ gel forming polymers. Preliminary studies using different ratios of pectin and guar gum were carried out to select a suitable ratio of both polymers. Each physical mixture was dissolved in 10 mL of 0.1 N HCl (pH 1.2) and the viscosity of the produced gel was measured using rotary viscometer with cone and plate (PK I-1°) as a sensor system (HAAKE, GmbH., Germany) at different shear rates. The viscosity and flow index (n) were calculated as done in our previous work.[27]

Formulation of ZT and ZT-NLC in in situ Gelling Hard Gelatin Capsule

ZT and ZT-NLC (F8) were formulated in in situ gelling hard gelatin capsules (size 0) using the proper ratio of pectin and guar gum. The ratio of both polymers was selected based on the results of viscosity. In a glass mortar, five mg of ZT were mixed by geometric proportion with 300 mg polymer mixture of the selected ratio. Subsequently, the prepared mixture was filled manually in hard gelatin capsules. Likewise, ZT-loaded NLC (F8) was prepared in the same manner using NLC equivalent to 5 mg ZT.

Evaluation of the Prepared Hard Gelatin Capsules

Uniformity of drug content: The USP 40 method was adopted[28] to calculate the drug content of the prepared capsules in 0.1 N HCl. The absorbance was measured at 282 nm.

In vitro release study: The in vitro release of ZT from the in situ gelling hard gelatin capsules was performed in triplicate via USP dissolution apparatus II, paddle method (Six-jars, USP, rotating paddle/basket, tablet dissolution test apparatus, DA-6D, India). In each vessel, one capsule was placed in 300 mL of 0.1 N HCl (pH 1.2) as a dissolution medium that was maintained at $37 \pm 0.5°C$ and rotated at 100 rpm. At definite time intervals (0.25, 0.5, 0.75, 1, 2, 3, 4, 5, 6, 7, 8, 24 and 30 h), aliquots of 3 mL were taken, filtered through 0.45 μm Millipore filter, then spectrophotometrically analyzed at 282 nm. After each sampling, an equal volume of fresh dissolution

medium was added. Placebo capsules were used as blanks. The percentage release of ZT was calculated as mean value ± SD.

Kinetic analysis: The release mechanism of ZT from the in situ gelling capsules was determined using zero-order, first-order,[29] Higuchi's equation[30] and Korsmeyer-Peppas semi-empirical model.[31]

Statistical Analysis

In vitro release results were calculated as mean ± S.D then were statistically analyzed via one-way analysis of variance (ANOVA), followed by post-test (DMRT test). The design of experiment (DOE) (2^3 full factorial design) was estimated respecting statistical significance through analysis of variance (ANOVA) via Design-Expert software (Design-Expert 11, State-Ease Inc., MN, USA). The principles for validation of the chosen model are statistically significant as p-value ($p < 0.05$) as well as the adjusted coefficients of determination (adjusted R^2) that lies between 0.8 and 1. Besides, the effect of CPPs on the different CQAs was demonstrated as a contour plot that was created by fixing one CPP and varying the two others over the range used in the study.

Pharmacodynamic Study
Animals

Adult male Swiss Albino mice, weighing between 25 and 30 g were used. Mansoura University Research Ethical Committee approved the protocol of animal use in agreement with "Principles of Laboratory Animal Care" (NIH publication No. 85–23, revised 1985).

Acetic Acid Induced Writhing Test

The animals were randomly allocated to four groups (a, b, c and d) (thirty mice/group); each group was subdivided into five subgroups (six mice/subgroup) for acetic acid injection at five time intervals (1, 2, 4, 6 and 8 h post drug administration), one subgroup for each interval. Another group comprising six mice served as the control group (group e).

Groups a and b received free ZT and NLCs (F8), respectively. On the other hand, ZT and NLC (F8), each of them in adjunct to pectin and guar gum (the components of in situ gelling capsules), were administered to groups c and d, respectively. The dose of free ZT or what is equivalent from NLC was 5mg/kg. The calculated dose of each treatment was suspended in de-ionized water (the volume was adjusted to 0.3 mL) and administered to mice

by oral gavage.[32] Likewise, the control group (e) administered 0.3 mL of normal saline. At each time interval (1, 2, 4, 6, and 8 h), hyperalgesia was induced in one of the five subgroups of each treatment via intraperitoneal injection of 0.3% acetic acid solution (10 mL/kg). Five min post acetic acid injection, the number of writhings was counted for 10 min. The injection of acetic acid to mice caused pain, which had been related to the pain experienced with migraine. For scoring purposes, a writhe is indicated by stretching of the abdomen with simultaneous stretching of at least one hind limb (Figure 1).[32,33] Percent inhibition in writhing was calculated using equation 3:[33]

$$\%inhibitions \ of \ writing = \frac{writing \ no \ in \ control \ group - writing \ no \ in \ Drug \ group}{writing \ no \ in \ Control \ group} x100$$

(3)

Statistical Analysis

The results of writhing number and the percentage inhibition of writhing for all groups of mice at the different time intervals were statistically analyzed using ANOVA, followed by post-test (DMRT) in order to compare between pairs. Computing the statistical analysis was carried out via IBM SPSS statistics 22.

Results and Discussion

Preliminary experiments highlighted the effect of variation in the amount of solid and liquid lipids together with the concentration of CT solution on the % EE and % yield of the prepared NLCs. The criteria for selection of NLC formulations by applying a full factorial design include high % EE, high % yield, low particle size, low PDI and high negative zeta potential. These CQAs are crucial touchstones to give indication for the efficacy as well as reproducibility of the processing technique. The optimum formula was found to be F8 which is composed of 150 mg of Gelucire, 0.15 mL of Labrasol and 1% w/v CT solution. No oral lipid nanoparticles (encompassing Gelucire and Labrasol) that dually fulfill the purpose of increasing permeability and prolonging the efficacy has been maneuvered for ZT.

Characterization and Optimization of ZT-Loaded NLCs by Full Factorial Design

On the basis of the defined constraints for each CPP, the Design Expert software automatically generated the optimized formula. The experimental values were obtained by preparing 8 batches of ZT loaded NLCs and simultaneously evaluating them for the predefined CQAs. The results of CQAs for various formulations have been detailed in Table 2.

The effect of CPPs on % EE, % yield, particle size, and DPI, were quantified through the polynomial coded equations. A positive value before the factor indicates that the response increases with this factor and vice versa for negative values.[34]

Percentage Entrapment Efficiency (% EE) and Percentage Yield (% Yield)

These two CQAs are considered a convenient red flag used to appraise the effectiveness as well as reproducibility of

Figure 1 Photography of writhing (stretching of the abdomen with simultaneous stretching of at least one hind) in mouse.

the processing technique. The obtained polynomial equations for these two CQAs are as follows:

% EE (R1) = + 56.19–6.54 A - 8.04 B + 4.11 C + 3.22 AB + 0.5350 AC - 1.30 BC - 0.7222 ABC (4)

Where F= 6164.85, p < 0.0001, and adjusted R^2=0.9995% yield (R2) = + 40.84–3.82 A - 3.40 B + 11.21 C + 4.31 AB + 0.9718 AC + 1.21 BC −1.198 ABC (5)

Where F= 1706.37, p < 0.0001, and adjusted R^2=1.000

Careful examination of these equations discloses that, only the concentration of CT solution (C) had a positive effect on % EE and % yield, while the other two CPPs (A and B) had a negative influence. Presumably, the hydrophilic drug (ZT) favored the partitioning in the external aqueous phase during preparation of NLC; thus increasing the lipids concentration in the formulation made the drug tend to escape to the aqueous phase with a decrease in the % EE. Hence, applying the technique of w/o/w double emulsion in the preparation of NLC helped in keeping ZT in the internal aqueous phase of the double emulsion.[32] Meanwhile, from the equations, it can be observed that the interaction of both terms (AB) demonstrated a positive effect. This can be explained by the fact that solid lipids in the NLC enclose liquid lipid sections that create tortuosity in a highly ordered crystal matrix, thus providing more void spaces for large amount of drug to be entrapped.[35]

To make it easy to interpret the power of different CPPs on the CQAs, the model equations for different CQAs were used to create several graphical plots. Figure 2 shows the contour plot of the above mentioned CQAs. CPPs, A (Gelucire amount) and B (Labrasol volume) were changed in the studied range while C (concentration of CT solution) was fixed at its high or low level.

The positive effect of CT on the % EE cannot be explained away from its positive effect on particle size. This means that the higher % EE that was observed with the higher concentration of CT solution was due to increasing the particle size of NLC which led to an increase in the overall accommodation space for the drug.[36] Interestingly, it can be observed from Table 2 and Figure 2 that the highest % EE and % yield occurred when A and B were at the lowest level while keeping C at the highest one (F8).

Particle Size Analysis and Polydispersity Index (PDI)

Regarding NLCs, not only their particle size (nm) but also their size distribution are crucial factors for evaluation. Particle size as well as size distribution are two important factors that influence the drug release rate, bioavailability and hence the pharmacodynamics of nanoparticles.

The particle size (nm) and PDI (a unitless quantity) of the prepared NLCs are shown in Table 2. From the obtained data, it is obvious that the PDI values of all NLCs were less than 0.3; this indicates a homogenous particle size distribution of all formulae.[37] It is worthknowing that, the lower the value of PDI (0.1 to 0.7), the more uniform the particle size distribution.[38]

Noticeably, Table 2 shows that F4 experienced the lowest value of particle size (209.33 nm) when all the CPPs were at their lowest levels. On the contrary, F5 experienced the highest particle size (666.93 nm) when all the CPPs were maintained at the highest levels. Together, the lowest value of particle size (F4) coincided with the lowest value of PDI. The synergistic effect of the three CPPs on particle size was interesting.

The obtained polynomial equations representing these two CQAs are as follows:

Particle size (R3) = + 347.75 + 62.21 A + 65.08 B + 88.41 C + 56.15 AB + 16.53 AC + 17.71 BC + 13.1 ABC (6)

Where F= 832.34, p < 0.0001, and adjusted R^2=0.9961

PDI (R4) = + 0.2003–0.0074 A + 0.0004 B + 0.0191 C - 0.0390 AB + 0.0026 AC - 0.0141 BC + 0.0104 ABC (7)

Where F= 25.43, p < 0.0001, and adjusted R^2=0.8814

These two equations divulge that, however the amount of Gelucire (A) had a negative effect on PDI, all the other CPPs had positive effect on particle size and PDI. Interestingly, the concentration of CT solution (C) demonstrated the highest coefficient. The increase in the particle size that occurred with increasing the amount of lipids (A and B) may be due to the aggregation of more particles, resulting in larger particle size.[39] Also, increasing the concentration of CT synergistically augmented this increase in particle size with a positive coefficient values of AB and ABC.

It can be inferred from Table 2 that an increase in the concentration of CT solution (C) from 0.3 to 1% w/v while keeping the other two CPPs (A and B) constant (F1 and F5, F2 and F6, F3 and F7, besides F4 and F8) had a positive effect on particle size. This may be due to increasing the viscosity of the aqueous phase by CT and a corresponding particle size increase.[40]
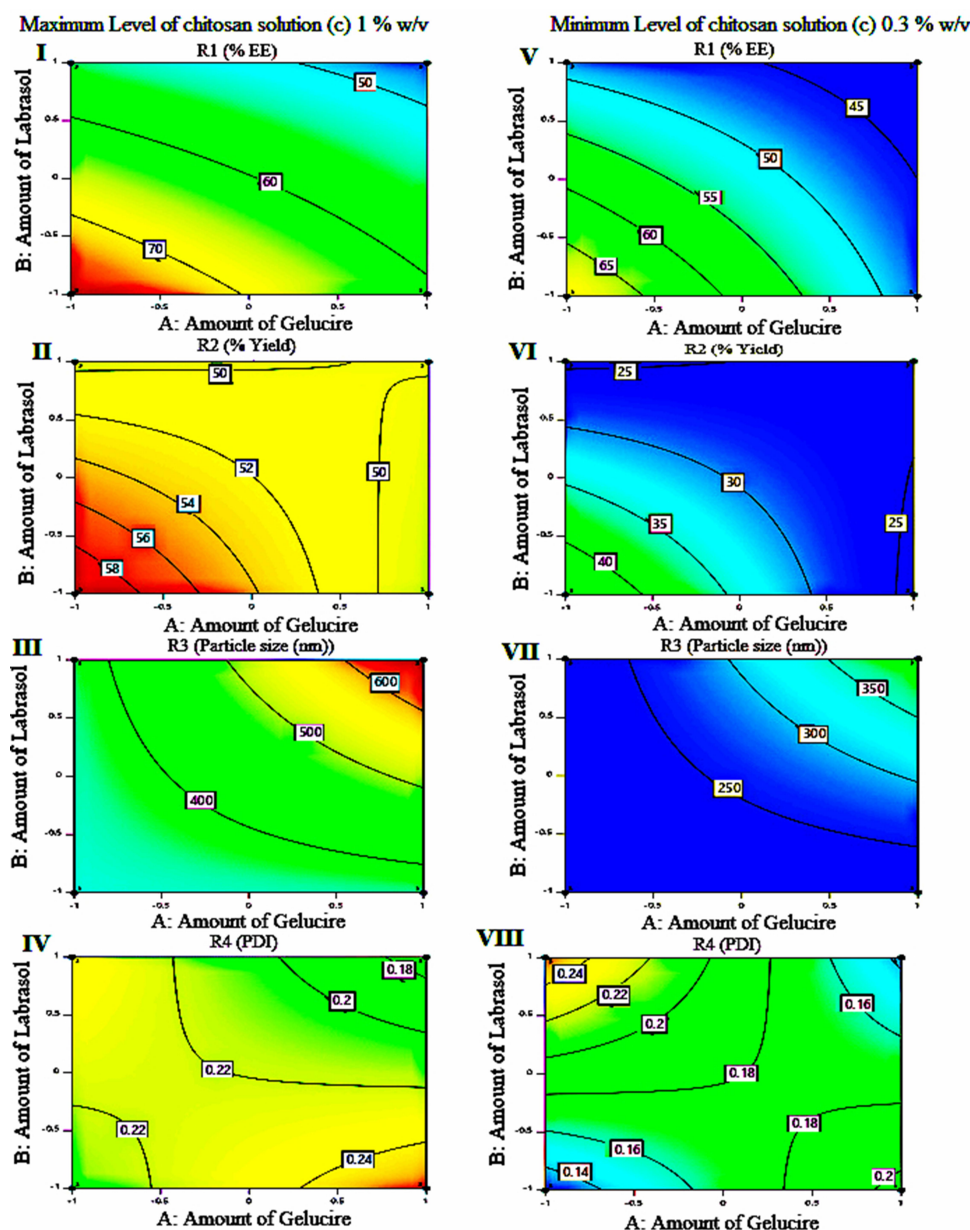
Figure 2 Contour plots showing the interaction between amounts of both gelucire (A) and labrasol (B) on % EE, % yield, particle size and PDI (I, II, III, and IV) and (V, VI, VII, and VIII) at the maximum and minimum level of chitosan solution concentration (c), respectively (Table 2).

It could be deduced from the aforementioned results that CT was the only CPP that had a positive effect on all studied CQAs. Hence, its inclusion in the NLC might help in augmenting the brain uptake potential of various drugs for targeting neurological disorders.[41] The desirability approach for optimization was set at low (particle size and PDI) and the highest (% EE and % yield). F8 with (A [−], B [−], C [+]) denoted the highest % EE, % yield, besides low particle size and PDI. This NLC formula would subsequently be subjected to further evaluations.

Evaluation of the Optimized ZT-Loaded NLC Formula (F8)

Zeta Potential (ZP) Determination

ZP is a common indicator for physical stability of aqueous nanodispersions. It indicates the degree of repulsion between close and similarly charged particles in the dispersion that plays a fundamental role in preventing aggregation of the particles. As the electrostatic repulsion between the particles increases, the stability increases. ZP was found to be −25.5 mV ± 0.1. This value was sufficiently high to obtain stable colloidal suspension

during preparation of NLC because the repulsive forces prevent aggregation with aging.[39] The negative charge was attributed to the anionic nature of the lipid and assured the higher lymphatic uptake.[42] The lymphatic uptake from negatively charged carriers was reported to be higher than neutral or positively charged surfaces.[43]

Transmission Electron Microscope (TEM)

TEM photograph discloses that the prepared NLCs exhibited spherical shape with perceptible lipid shell and a core encapsulating ZT (multi-layered NLC). The homogeneous monolayer surface coating with Tween 80 at the periphery of the NLC particles surrounding the lipid core could be clearly seen (Figure 3). Being amphiphilic in character, Tween 80 was adsorbed on the surface of NLCs. The stabilization effect of Tween 80 cannot be ignored.

Fourier Transform Infrared Spectroscopy (FTIR)

Figure 4A showed the FTIR spectra of ZT. The spectra demonstrated the characteristic bands at 3351, 1737, 1409 and 1259 cm^{-1} owing to N–H, C=O, C=C, and C–O stretching vibration, respectively.[32,44] In the FTIR spectrum of Gelucire (Figure 4B), the distinct absorption bands at 2851 and 1119 cm^{-1} were attributed to C-H and C-O (ether) stretching vibration, respectively.[45] It also exhibited two characteristic bands at 1734 and 2918 cm^{-1} due to carbonyl and hydroxyl group (O-H) stretching, respectively. Besides, the band at 1469 cm^{-1} was due to C-H deformation of alkyl group.[46]

The FTIR spectrum of CT (Figure 4C) showed two distinct bands at 1543 as well as 1649 cm^{-1} denoting N-H bending vibration of amino groups and carbonyl stretching vibration of the secondary amide group,
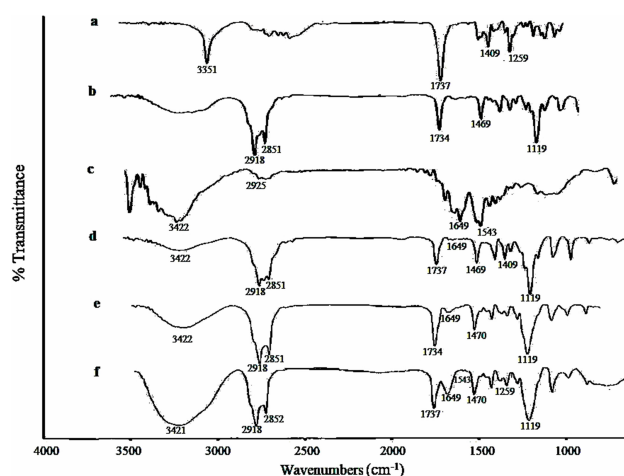

Figure 4 FTIR spectra of: (a) ZT, (b) Gelucire, (c) CT, (d) Gelucire, CT and ZT physical mixture, (e) Plain NLC and (f) ZT-loaded NLC (F8).

respectively.[27] The band at 2925 cm^{-1} was due to C-H stretching vibration.[47] Besides, the band at 3422 cm^{-1} was due to OH stretching, indicating intermolecular hydrogen bonding of CT molecules.[48]

The spectrum of ZT, Gelucire and CT physical mixture (Figure 4D) showed the bands of the individual components except those of the drug. The characteristic absorption bands of ZT (N–H and C–O) disappeared while those of C=O and C=C were with small intensities. This might be attributed to the dilution effect. Likewise, the spectra of the plain NLC (Figure 4E) and ZT loaded NLC (Figure 4F) coincided with those of the individual ones except the absence of ZT bands in the plain NLC. This means the absence of interaction between ZT and other ingredients. Also, this established the entrapment of ZT in the lipid matrix.
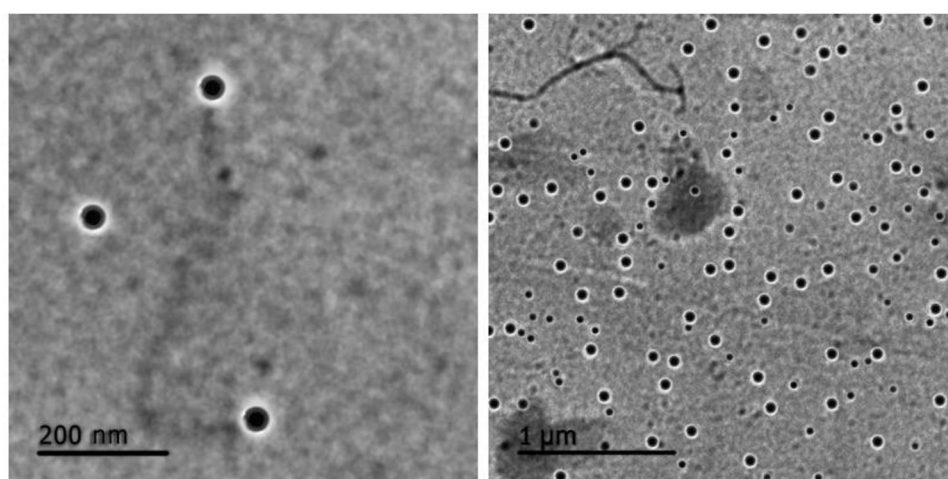

Figure 3 TEM image of the optimized ZT-loaded NLC with low level of gelucire, labrasol and high level of concentration of CT solution (F8, Table 2).
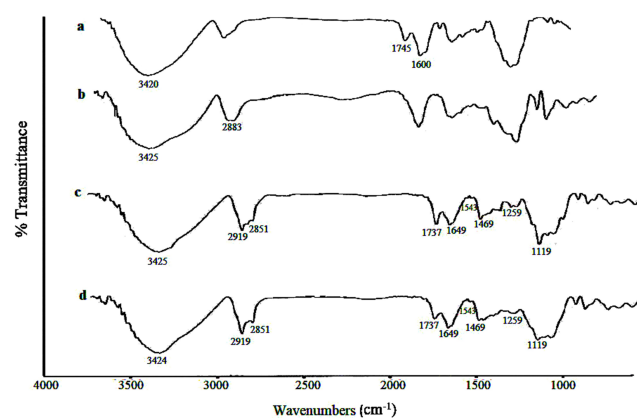
Figure 5 FTIR spectra of: (a) Pectin, (b) Guar gum, (c) Physical mixture of ZT, Gelucire, CT, pectin and guar gum, and (d) Mixture of ZT-loaded NLC (F8) with pectin and guar gum.

Figure 5A showed the characteristic absorption bands of pectin. The distinct broad absorption band at 3420 cm^{-1} typifies the O-H group. Another stretching bands for carboxylic acid and C=O of methyl ester groups appeared at 1600 and 1745 cm^{-1} respectively.[49,50] Guar gum spectrum (Figure 5B) showed a distinctive broad absorption band at 3425 cm^{-1} (due to O-H stretching) and 2883 cm^{-1} (due to aliphatic C-H stretching).[51]

The spectra of either physical mixture of ZT, Gelucire, CT, pectin and guar gum or mixture of NLC representing

F8 with pectin and guar gum (Figure 5C and D) showed similar absorption patterns. The absence of ZT bands in these two spectra might be due to either masking of the drug by the comparatively large amount of polymers (Gelucire, pectin and guar gum) or the drug entrapment in the lipid matrix.

Differential Scanning Colorimetry (DSC)

DSC was performed to investigate the melting and crystallization behavior of the drug, lipid and other polymers used in the nanoparticle preparations.

A sharp endothermic peak at 140°C was observed. This peak corresponds to the melting point of ZT (Figure 6A) which indicates the crystalline nature of untreated ZT.[44] Gelucire exhibited two endothermic peaks at 48 and 52°C (Figure 6B).[52,53] The broad endothermic peak of CT at 87°C in Figure 6C was attributed to dehydration of the polymer and loss of water associated with the hydrophilic O-H group of the amorphous CT.

Pectin showed endothermic peaks at 66.5, 244.5, 306.8 and 350.2°C (Figure 6D).[54] The DSC curve of guar gum (Figure 6E) showed a melting endotherm at 239.5°C which indicates its crystalline nature.[55] Another broad endothermic peak appeared at 80°C corresponding to the hydrophilic groups O-H group.
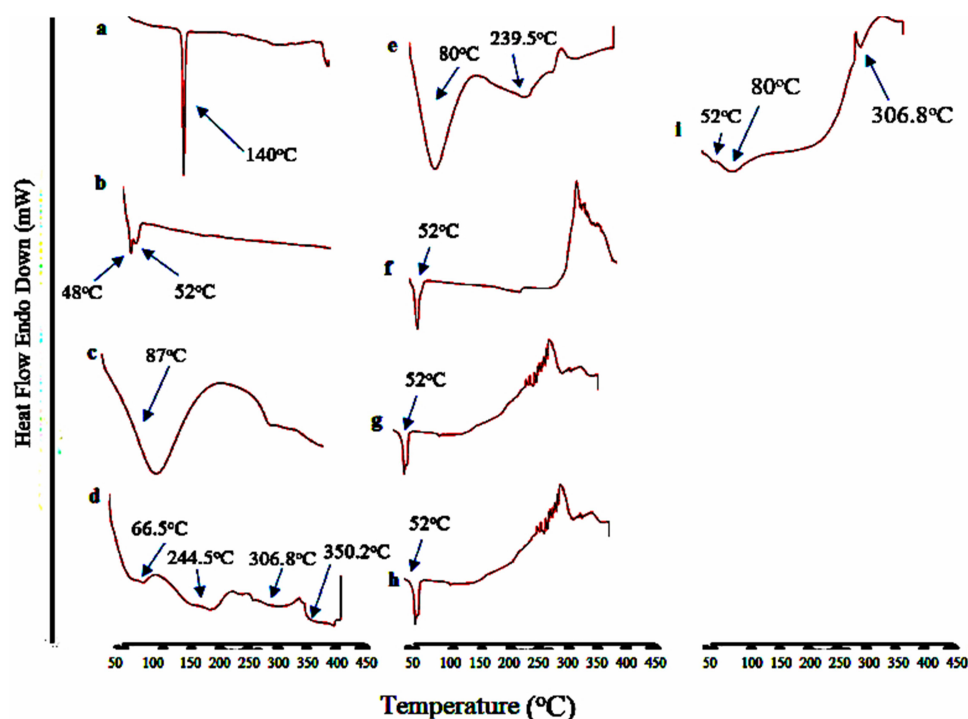

Figure 6 DSC thermograms of: (a) ZT, (b) Gelucire, (c) CT, (d) Pectin, (e) Guar gum, (f) Mixture of ZT, gelucire and CT, (g) Plain NLC, (h) ZT- loaded NLC (F8), and (i) Mixture of ZT-loaded NLC (F8) with pectin and guar gum.

The endothermic peak of ZT was absent in the thermograms of its physical mixture with Gelucire and CT, ZT loaded NLC representing F8 and mixture of F8 with pectin and guar gum (Figure 6F, H, and I, respectively). This might be attributed to either the dispersion of ZT within the lipid matrix or the presence of ZT in the amorphous form. The absence of CT peak in the thermograms of its physical mixture with ZT and Gelucire, plain NLC and ZT-loaded NLC (F8) may be due to masking of the CT peak by the comparatively large amount of Gelucire (Figure 6F–H respectively). Figure 6I showed endothermic peaks at 52, 80 and 306 °C corresponding to Gelucire, guar gum and pectin respectively.

The results of DSC studies support the IR spectroscopy results for the absence of interaction between the used ingredients.

Stability Study of the Optimized Formula (F8)

F8 was selected as the optimized formula on the basis of all the aforementioned results. It had the highest % EE, high % yield together with low particle size and PDI. F8 was physically unchanged and showed no phase separation at ambient or refrigerated conditions indicating good physical stability.

The statistical analysis of the results of % EE, particle size, PDI and ZP revealed an insignificant difference in either particle size or PDI during storage at refrigerated condition (p>0.05). However, they showed a significant increase when stored at ambient conditions (p<0.001 and p<0.01, respectively) (Table 3) which may be attributed to particle collision. These results pointed out that the optimized formula (F8) was stable when stored at refrigerated condition for 3 months, where the

nanosize range together with homogenous particle distribution prevailed.

Formulation of the Optimized ZT-NLCs (F8) in in situ Gelling Hard Gelatin Capsule

The criteria for selection of polymers for developing in situ gelling capsule include pharmaceutical acceptability, biodegradability, non-toxicity and capability to form in situ gel with high viscosity through which the drug is released in a sustained manner.

As per the results of viscosity at different shear rates for different ratios of pectin and guar gum (Table 4), it can be noted that, the higher the ratio of guar gum in the mixture, the higher the viscosity of the gel. Also, the addition of pectin enhanced the viscosity. This synergistic interaction could be due to the interactions between the helix forming polysaccharide (pectin) and (1-4)-β-D mannans.[56] Moreover, as the shear rate increased, the viscosity of the gel (at all pectin: guar gum ratio) decreased. Thus, all the formed gels exhibited pseudoplastic (shear thinning) behaviour. This was further supported by the flow index values (n), which were found to be less than 1 augmenting the shear thinning behaviour (Table 4). Based on this rheological study, pectin and guar gum were used as in situ gel forming polymers at a ratio of 1:4 in hard gelatin capsule.

Evaluations of the Prepared Hard Gelatin Capsules

Uniformity of Drug Content

The drug content of the prepared hard gelatin capsules for free ZT and NLC (each with pectin and guar gum) was found to be 98.85 ± 0.54 and 96.76 ± 2.83, respectively.

Table 3 Particle Size, PDI, ZP and Drug Retention % of ZT-Loaded NLC Aqueous Dispersions (F8) Stored at Refrigerated (5 ± 3°C) and Ambient (25 ± 2°C/40 ± 5% RH) Conditions (See Table 2 for F8 Composition)

Storage Time	Evaluation Parameters							
	Refrigerated Temperature (5 ± 3 °C)				Ambient Temperature (25 ± 2 °C/40% RH ± 5%)			
	Particle Size (nm)	PDI	ZP (mV)	Drug Retention (%)	Particle Size (nm)	PDI	ZP (mV)	Drug Retention (%)
Zero time	394.17 ± 23.45	0.129 ± 0.092	−27.59± 0.1	100 ± 0.00	394.17 ± 23.45	0.129 ± 0.092	−27.59 ± 0.1	100 ± 0.00
1 month	382.23 ± 23.41	0.193 ± 0.029	−25.23± 0.87	99.17 ± 0.81	741.67 ± 10.41***	0.265 ± 0.014	−16.17 ± 0.5***	97.89 ± 2.31
2 months	349.73 ± 5.87	0.186 ± 0.028	−21.52± 2.54***	98.17 ± 8.29	817.42 ± 19.73***	0.35 ± 0.068**	−12.47 ± 0.15***	97.42 ± 7.63
3 months	377.75 ± 19.21	0.135 ± 0.054	−24.23± 0.33	98.92 ± 3.22	947.32 ± 10.43***	0.38 ± 0.039**	−14.82 ± 0.26***	95.61 ± 4.21

Notes: Each measurement was mean of three determinations ± S.D. **Highly significant at p < 0.01 monthly vs initial. ***Extremely significant at p < 0.001 monthly vs initial.

Table 4 Mean Viscosities of Different Ratios of Pectin/Guar Gum Physical Mixtures in 0.1N HCl of pH 1.2

Pectin:Guar Gum Ratio	*Viscosity (mpa.s) at Shear Rate 192 s^{-1} (32 rpm) ± SE	*Viscosity (mpa.s) at Shear Rate 384 s^{-1} (64 rpm) ± SE	*Viscosity (mpa.s) at Shear Rate 768 s^{-1} (128 rpm) ± SE	*Flow Index (n) at Shear Rate 768 ± SE
1: 1	5251.04 ± 73.96	536.198 ± 46.67	27.73 ± 2.01	0.204 ± 0.003
2: 1	6397.39 ± 133.33	776.58 ± 64.05	92.45 ± 8.49	0.355 ± 0.005
3: 1	6804.17 ± 147.92	1035.42 ± 73.96	101.69 ± 9.25	0.358 ± 0.0019
4: 1	6878.13 ± 128.1	1257.29 ± 73.96	147.92 ± 10.49	0.411 ± 0.004
Pure pectin	4881.25 ± 18.49	517.71 ± 6.75	18.49 ± 8.49	0.153 ± 0.008
1: 2	7469.79 ± 73.96	1442.19 ± 64.05	160.12 ± 6.82	0.326 ± 0.003
1: 3	8283.33 ± 147.92	1664.06 ± 64.05	184.89 ± 16.98	0.415 ± 0.006
1: 4	9318.75 ± 256.199	2126.3 ± 66.67	314.32 ± 18.49	0.476 ± 0.003
Pure guar gum	8653.13 ± 16.98	1885.94 ± 73.96	295.83 ± 14.05	0.479 ± 0.003

Notes: *Mean of three determinations ± S.E.

The obtained results ensure good drug content uniformity in the capsules.

In vitro Release Study

Figure 7 shows the release profiles of the optimized NLC (F8) and the free ZT in hard gelatin capsule, both without the in situ gelling polymers. It can be observed that both ZT, whether free or in NLC (F8), experienced burst effect. Free ZT exhibited complete release within 30 min, while in case of NLC, it took about 5h. This may be attributed to the formation of hydrogen bond between either the (C=O) or amino group (NH) of the drug and water molecules, allowing migration of surface molecules of ZT.[36]

However, the in vitro release profile from in situ gelling capsule was distinguishable. ZT in in situ gelling capsule showed biphasic pattern. A negligible release prevailed for 2 h, then, about 50% of ZT was released over 6 h. The remaining drug was released at a slower rate within 24 h. This bi-phasic pattern of release is a characteristic
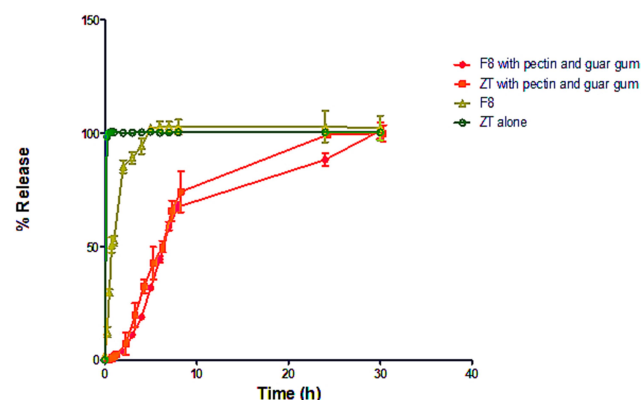

Figure 7 Dissolution of ZT in 0.1 N HCl (pH 1.2) from: Free ZT (○) and F8 (Δ) without polymers in hard gelatin capsules, ZT with pectin and guar gum (●) and F8 with pectin and guar gum (■).

feature of matrix diffusion kinetics. This might be attributed to the disentanglement of the roughly bound molecules due to the rapid hydration and erosion of the matrix. Moreover, the polymer matrix lost its integrity via relaxation when swelled in 0.1 N HCl; the drug dissolved and diffused out because of concentration gradient.[27] This also cannot be explained away from the rheological characteristics of the in situ gelling polymers, where the viscous matrix led to increase the tortuosity of the diffusion pathway that the drug molecules had to cross.[57] This emphasizes no dose dumping from the in situ gelling hard gelatin capsule. Hence, pectin and guar gum were used at a ratio of 1:4 owing to their highest viscosity (Table 4).

To the author's knowledge, the idea of a synergistic effect of both NLC and in situ gelling system that could effectively sustain ZT effect for better efficacy by oral route has not been allocated before. In light of this contemplation, the formulation of ZT-NLC in in situ gelling hard gelatin capsule was carried out. Interestingly, NLC in in situ gelling hard gelatin capsule comprising pectin and guar gum experienced the most sustainable drug release for 30 h compared to free ZT with pectin and guar gum (Figure 7).

From the aforementioned results, it can be concluded that ZT-NLC with in situ gelling polymers is an optimized dosage form for oral delivery of ZT. The forthcoming in vivo results will verify this conclusion.

Kinetic Analysis

It is revealed from the r^2 values that zero order release is prevailed (Table 5). The results of the exponential (n) in Korsmeyer-Peppas equation were found to be (n > 1) in all formulae indicating anomalous (non-Fickian) release mechanism (super case II). This suggested that both

Table 5 Mathematical Modeling and Release Kinetics of the Prepared Hard Gelatin Capsule

Formula Code	Zero-Order Plots Correlation Coefficient (r^2)	First-Order Plots Correlation Coefficient (r^2)	Higuchi's Plots Correlation Coefficient (r^2)	Korsmeyer–Peppas Plots		
				Correlation Coefficient (r^2)	Diffusional Exponent (n)	Mechanism of Release
F8	0.9825	0.9496	0.8754	0.9430	1.22 ± 0.09	Zero order (super case II)
ZT with pectin and guar gum	0.9906	0.9624	0.8434	0.9797	1.745 ± 0.05	Zero order (super case II)
ZT loaded NLC (F8) with pectin and guar gum	0.9974	0.9304	0.7752	0.9863	1.763 ± 0.04	Zero order (super case II)

diffusion of the drug from the hydrated matrix and its own erosion modulate the drug release. The matrix erosion in case of F8 resulted from degradation of lipids.

Pharmacodynamic Study

The number of writhings in mice after administration of the suggested formulae (F8 [NLC alone], free ZT with pectin and guar gum and NLC with pectin and guar gum) was statistically analyzed and the results were shown in Figure 8. Free ZT was included for comparison (group a). Control group received only normal saline (group e). It can be observed in Figure 8 that the number of writhings for the investigated groups was quite different (p < 0.05) and the maximum effect of all groups was noticed after 4 h. Kalanuria and Peterlin observed a maximum reduction in rates of

photophobia (migraine symptom) at 4 h after ZT administration.[58]

It could be further observed from Figure 8 that all groups showed a decrease in the number of writhings (analgesic effect) compared to the control group. Careful examination of Figure 8 disclosed the effect of formulating ZT in NLC (group b) on its pharmacodynamics when compared with free ZT (group a). This effect may be due to impending ZT rapid uptake as well as metabolism by liver cells, enhancing its pharmacodynamic effect.

The corresponding values of group c (free ZT and polymers) revealed that no significant reduction in the writhing number was observed when compared with group a (free ZT) for the first 4 h (p > 0.05); after this time, the effect was significant. It is worth noting that dispensing NLC in in situ gelling hard gelatin capsule
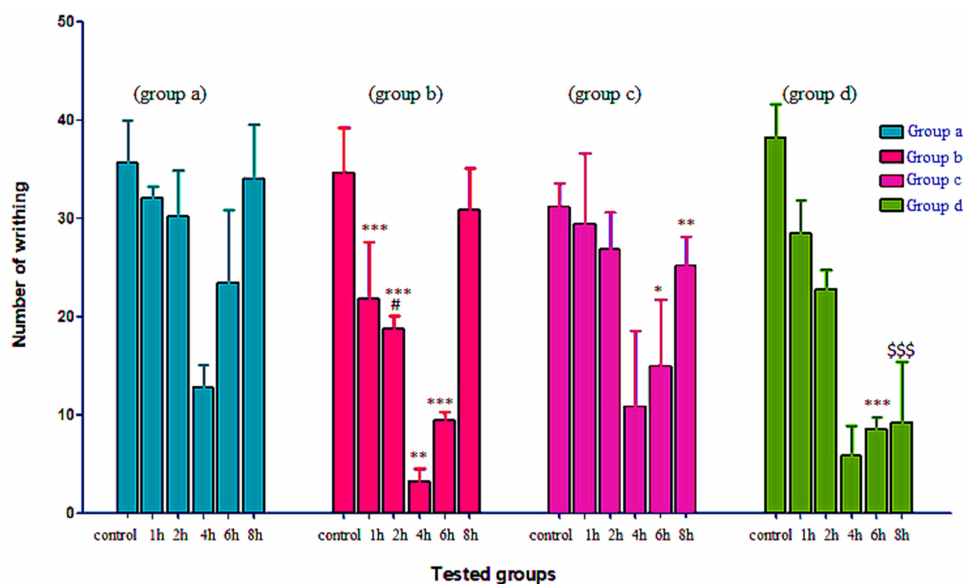

Figure 8 Effect of free ZT (group a), ZT loaded NLC [F8] (group b), ZT in in situ gelling hard gelatin capsule (group c), ZT-loaded NLC in in situ gelling hard gelatin capsule (group d) and control groups (normal saline) on the number of writhings after induction with acetic acid in mice at different time intervals.
Notes: *P<0.05, **p<0.01 and ***p<0.001 vs group a. #P<0.05 vs group c. $$$p<0.001 vs groups a, b and c.

(group d) significantly maintained the pharmacodynamic effect up to 8 h (p < 0.001). Herein, the aim of this research has been fulfilled.

The above results inferred that NLC improved ZT efficacy through dual tackling of its poor permeability and pre-systemic metabolism. The effect of CT in NLC as penetration enhancer cannot be ignored.[19] Also, coating the surface of NLC particles with Tween 80 had a similar effect on membrane permeability.[59] Surface coating with Tween 80 provides stealth characters to the particles preventing opsonization.[60] Meanwhile, in situ gelling system with high viscosity helped in sustaining the drug release. Based on these findings, the net result would be improving ZT efficacy.[61]

Conclusions

Quality by design (QbD) approach has been adopted to optimize three CPPs (amount of Gelucire [A], volume of Labrasol [B] and concentration of chitosan solution [C]) for preparing NLCs with high percentage of EE and yield and with low particle size and PDI. The optimized prepared NLC (F8) has sufficient charge (zeta potential) to inhibit vesicle aggregation. TEM imaging of the freshly prepared F8 illustrated the homogeneous monolayer coating of surfactant (Tween 80) at the periphery, which provides stealth characters to the particles and improves membrane permeability. The NLC was dispensed in hard gelatin capsule encompassing in situ gel forming polymers, thus sustaining ZT release for more than 24 h. The pharmacodynamic effect of the NLC (F8) in mice was statistically different from that of the plain drug. Beside the improved efficiency, the NLCs were more sustainable. BCS class III drugs with poor permeability can be prepared in lipid nanoparticles encompassing penetration enhancer to improve their efficiency. QbD approach seems to be an efficient way to optimize the critical process parameters.

Disclosure

The authors report that this manuscript is based on the Masters thesis of the first author (Randa Hanie Awadeen). The second author (Mariza Fouad Boughdady) and the third author (Mahasen Mohamed Meshali) were supervisors. The authors report no conflicts of interest for this work.

References

1. Shah NV, Seth AK, Balaraman R, et al. Nanostructured lipid carriers for oral bioavailability enhancement of raloxifene design and in vivo study. *J Adv Res*. 2016;7:423–434. doi:10.1016/j.jare.2016.03.002
2. Prajapati ST, Patel MV, Patel CN. Preparation and evaluation of sublingual tablets of Zolmitriptan. *Int J Pharm Investig*. 2014;4 (1):27–31. doi:10.4103/2230-973X.127737
3. Moffat AC, Osselton MD, Widdop B, Watts J. *Clarke's. Analysis of Drugs and Poisons in Pharmaceuticals Body Fluids and Post-Mortem Material*. 4th. London, UK: The pharmaceutical press; 2011: 1462–2253
4. Abd-Elal RM, Shamma RN, Rashed HM, Bendas ER. Trans-nasal Zolmitriptan novasomes: in-vitro preparation, optimization and in-vivo evaluation of brain targeting efficiency. *Drug Deliv*. 2016;23 (9):3374–3386. doi:10.1080/10717544.2016.1183721
5. El-Nabarawy NA, Teaima MH, Helal DA. Assessment of spanlastic vesicles of zolmitriptan for treating migraine in rats. *Drug Des Devel Ther*. 2019;13:3929–3937. doi:10.2147/DDDT.S220473
6. Pitta SK, Dudhipala N, Narala A, Veerabrahma K. Development of zolmitriptan transfersomes by Box-Behnken design for nasal delivery: in vitro and in vivo evaluation. *Drug Dev Ind Pharm*. 2018;44 (3):484–492. doi:10.1080/03639045.2017.1402918
7. Imam SS, Ahad A, Aqil M, Akhtar M, Sultana Y, Asgar A. Formulation by design based risperidone nano soft lipid vesicle as a new strategy for enhanced transdermal drug delivery: in-vitro characterization, and in-vivo appraisal. *Mater Sci Eng*. 2017;75:1198–1205. doi:10.1016/j.msec.2017.02.149
8. Imam SS, Aqil M, Akhtar M, Sultana Y, Ali A. Formulation by design-based proniosome for accentuated transdermal delivery of risperidone: in vitro characterization and in vivo pharmacokinetic study. *Drug Deliv*. 2015;22(8):1059–1070. doi:10.3109/10717544.2013.870260
9. Alam M, Zameer S, Najmi A, Ahmad FJ, Imam SS, Akhtar M. Thymoquinone loaded solid lipid nanoparticles demonstrated antidepressant-like activity in rats via indoleamine 2, 3- dioxygenase pathway. *Drug Res*. 2020;70(5):206–213. doi:10.1055/a-1131-7793
10. Chauhan I, Yasir M, Verma M, Singh AP. Nanostructured lipid carriers: a groundbreaking approach for transdermal drug delivery. *Adv Pharm Bull*. 2020;10(2):150–165. doi:10.34172/apb.2020.021
11. Shah SM, Jain AS, Kaushik R, Nagarsenker MS, Nerurkar MJ. Preclinical formulations: insight, strategies, and practical considerations. *AAPS Pharm Sci Tech*. 2014;15:1307–1323. doi:10.1208/s12249-014-0156-1
12. McCartney F, Jannin V, Chevrier S, et al. Labrasol® is an efficacious intestinal permeation enhancer across rat intestine: ex vivo and in vivo rat studies. *J Control Release*. 2019;310:115–126. doi:10.1016/j.jconrel.2019.08.008
13. Panigrahi KC, Patra CN, Jena GK, et al. Gelucire: a versatile polymer for modified release drug delivery system. *FJPS*. 2018;4:102–108.
14. Tamjidi F, Shahedi M, Varshosaz J, Nasirpour A. Nanostructured lipid carriers (NLC): a potential delivery system for bioactive food molecules. *Innov Food Sci Emerg Technol*. 2013;19:29–43. doi:10.1016/j.ifset.2013.03.002
15. Samy W, Elgindy N, El-Gowelli HM. Biopolymeric nifedipine powder for acceleration of wound healing. *Int J Pharm*. 2012;422:323–331. doi:10.1016/j.ijpharm.2011.11.021
16. Mohammed MA, Syeda JTM, Wasan KM, Wasan EK. An overview of chitosan nanoparticles and its application in non-parenteral drug delivery. *Pharmaceutics*. 2017;9(4):53–78. doi:10.3390/pharmaceutics9040053
17. Razmi M, Divsalar A, Saboury AA, Izadi Z, Haertlé T, Mansuri-Torshizi H. Beta-casein and its complexes with chitosan as nanovehicles for delivery of a platinum anticancer drug. *Colloids Surf B*. 2013;112:362–367. doi:10.1016/j.colsurfb.2013.08.022

18. Sacco P, Furlani F, Marzo G, Marsich E, Paoletti S, Donati I. Concepts for developing physical gels of chitosan and of chitosan derivatives. *Gels*. 2018;4:67–95. doi:10.3390/gels4030067

19. Bernkop-Schnürch A, Dünnhaupt S. Chitosan-based drug delivery systems. *Eur J Pharm Biopharm*. 2012;81:463–469. doi:10.1016/j.ejpb.2012.04.007

20. Prakash K, Satyanarayana V, Nagiat H, Fathi A, Shanta A, Prameela A. Formulation, development and evaluation of novel oral jellies of carbamazepine using pectin, guar gum, and gellan gum. *Asian J Pharm*. 2014;8(4):241–249. doi:10.4103/0973-8398.143937

21. Wu Y, Liu Y, Li X, et al. Research progress in in-situ gelling ophthalmic drug delivery system. *AJPS*. 2019;14(1):1–15.

22. Kushwaha AK, Vuddanda PR, Karunanidhi P, Singh SK, Singh S. Development and evaluation of solid lipid nanoparticles of Raloxifene hydrochloride for enhanced bioavailability. *Biomed Res Int*. 2013;2013(8):1–9. doi:10.1155/2013/584549

23. Aman RM, Abu Hashim II, Meshali MM. Novel chitosan-based solid-lipid nanoparticles to enhance the bio-residence of the miraculous phytochemical "Apocynin". *Eur J Pharm Sci*. 2018;124:304–318. doi:10.1016/j.ejps.2018.09.001

24. Nair R, Kumar AC, Priya VK, Yadav CM, Raju PY. Formulation and evaluation of chitosan solid lipid nanoparticles of Carbamazepine. *Lipids Health Dis*. 2012;11:1–8. doi:10.1186/1476-511X-11-72

25. Shah M, Agrawal Y, Garala K, Ramkisha A. Solid lipid nanoparticles of a water soluble drug, Ciprofloxacin hydrochloride. *Indian J Pharm Sci*. 2012;74(5):434–442. doi:10.4103/0250-474X.108419

26. El-Housiny S, Shams Eldeen MA, El-Attar YA, et al. Fluconazole-loaded solid lipid nanoparticles topical gel for treatment of pityriasis versicolor: formulation and clinical study. *Drug Deliv*. 2018;25(1):78–90. doi:10.1080/10717544.2017.1413444

27. Awadeen RH, Boughdady MF, Meshali MM. New in-situ gelling biopolymer-based matrix for bioavailability enhancement of glimepiride; in-vitro/in-vivo x-ray imaging and pharmacodynamic evaluations. *Pharm Dev Technol*. 2019;24(5):539–549. doi:10.1080/10837450.2018.1517366

28. USP. *The United States Pharmacopeia*. 40th ed. Twinbrook parkway, Rockville: The United States Pharmacopeial Convention; 2017.

29. Sinko PJ. Chemical kinetics and stability. In: *Martin's Physical Pharmacy and Pharmaceutical Sciences*. 6th ed. Lippincott Williams and Wilkins; 2011:318–354.

30. Higuchi T. Mechanism of sustained-action medication: theoretical analysis of rate of release of solid drugs dispersed in solid matrices. *J Pharm Sci*. 1963;52(12):1145–1149. doi:10.1002/jps.2600521210

31. Peppas N. Analysis of Fickian and non-Fickian drug release from polymers. *Pharm Acta Helv*. 1985;60:110–111.

32. Girotra P, Singh SK, Kumar G. Development of Zolmitriptan loaded PLGA/poloxamer nanoparticles for migraine using quality by design approach. *Int J Biol Macromol*. 2016;85:92–101. doi:10.1016/j.ijbiomac.2015.12.069

33. Abdelkader H, Abdallah OY, Salem HS. Comparison of the effect of tromethamine and polyvinylpyrrolidone on dissolution properties and analgesic effect of nimesulide. *AAPS Pharm Sci Tech*. 2007;8(3):E1–E8. doi:10.1208/pt0803065

34. Thakkar HP, Desai JL, Parmar MP. Application of Box-Behnken design for optimization of formulation parameters for nanostructured lipid carriers of Candesartan cilexetil. *Asian J Pharm*. 2014;8:81–89. doi:10.4103/0973-8398.134921

35. Dudhipala N, Janga KY, Gorre T. Comparative study of nisoldipine-loaded nanostructured lipid carriers and solid lipid nanoparticles for oral delivery: preparation, characterization, permeation and pharmacokinetic evaluation. *Artif Cell Nanomed Biotechnol*. 2018;46(Suppl 2):616–625. doi:10.1080/21691401.2018.1465068

36. Gaba B, Fazil M, Khan S, Ali A, Baboota S, Ali J. Nanostructured lipid carrier system for topical delivery of Terbinafine hydrochloride. *Bull Fac Pharm Cairo Univ*. 2015;53:147–159. doi:10.1016/j.bfopcu.2015.10.001

37. Elmowafy M, Ibrahim HM, Ahmed MA, Shalaby K, Salama A, Hefesha H. Atorvastatin-loaded nanostructured lipid carriers (NLCs): strategy to overcome oral delivery drawbacks. *Drug Deliv*. 2017;24(1):932–941. doi:10.1080/10717544.2017.1337823

38. Rajinikanth PS, Chellian J. Development and evaluation of nanostructured lipid carrier-based hydrogel for topical delivery of 5-fluorouracil. *Int J Nanomed*. 2016;11:5067–5077. doi:10.2147/IJN.S117511

39. Dandagi PM, Dessai GA, Gadad AP, Desai VB. Formulation and evaluation of nanostructured lipid carrier (NLC) of lornoxicam. *Int J Pharm Pharm Sci*. 2014;6(2):73–77.

40. Choi KO, Choe J, Suh S, Ko S. Positively charged nanostructured lipid carriers and their effect on the dissolution of poorly soluble drugs. *Molecules*. 2016;21:2–12. doi:10.3390/molecules21050672

41. Tapeinos C, Battaglini M, Ciofani G. Advances in the design of solid lipid nanoparticles and nanostructured lipid carriers for targeting brain diseases. *J Control Release*. 2017;264:306–332. doi:10.1016/j.jconrel.2017.08.033

42. Wang K, Zhang QJ, Miao YL, Luo SQ, Wang HC, Zhang WP. Effect of solid lipid's structure on nanostructured lipid carriers encapsulated with sun filter: characterization, photo-stability and in-vitro release. *J Microencapsul*. 2017;34(1):104–110. doi:10.1080/02652048.2017.1290156

43. Khan AA, Mudassir J, Mohtar N, Darwis Y. Advanced drug delivery to the lymphatic system: lipid-based nanoformulations. *Int J Nanomedicine*. 2013;8:2733–2744.

44. Mandlik SK, Adhikari S, Ranpise NS. Formulation and in-vitro characterization of chitosan biodegradable nanoparticles of Zolmitriptan for migraine treatment. *Pharm Glob*. 2013;4(1):1–5.

45. El Hadri M, Achahbar A, El Khamkhami J, Khelifa B. Vibrational behavior of Gelucire 50/13 by Raman and IR spectroscopies: a focus on the 1800–1000cm^{-1} spectral range according to temperature and degree of hydration. *J Mol Struct*. 2015;1083:441–449. doi:10.1016/j.molstruc.2014.10.062

46. Sharma N, Singh S. Central composite designed ezetimibe solid dispersion for dissolution enhancement: synthesis and in vitro evaluation. *Ther Deliv*. 2019;10(10):643–658. doi:10.4155/tde-2019-0063

47. Rumengan IFM, Suryanto E, Modaso R, Wullur S, Tallei TE, Limbong D. Structural characteristics of chitin and chitosan isolated from the biomass of cultivated rotifer, brachionus rotundiformis. *Int J Fish Aquat Stud*. 2014;3(1):12–18.

48. Zhong Q, Wu Z, Qin Y, et al. Preparation and properties of carboxymethyl chitosan/alginate/tranexamic acid composite films. *Membranes*. 2019;9:11–18. doi:10.3390/membranes9010011

49. Pramanik D, Ganguly M. Formulation and evaluation of a pectin based controlled drug delivery system containing Metronidazole. *RJLBPCS*. 2017;3(4):16–25.

50. Copikova J, Synytsya A, Cerna M, Kaasova J, Novotna M. Application of FT-IR spectroscopy in detection of food hydrocolloids in confectionery jellies and food supplements. *Czech J Food Sci*. 2008;19(2):51–56. doi:10.17221/6575-CJFS

51. Khan K, Naeem M, Ali A, et al. Assessment of guar and xanthan gum based floating drug delivery system containing mefenamic acid. *Acta Pol Pharm*. 2016;73(5):1287–1297.

52. Eloy JDO, Saraiva J, Albuquerque SD, Marchetti JM. Solid dispersion of ursolic acid in gelucire 50/13: a strategy to enhance drug release and trypanocidal activity. *AAPS Pharm Sci Tech*. 2012;13(4):1436–1445. doi:10.1208/s12249-012-9868-2

53. Date AA, Vador N, Jagtap A, Nagarsenker MS. Lipid nanocarriers (GeluPearl) containing amphiphilic lipid Gelucire 50/13 as a novel stabilizer: fabrication, characterization and evaluation for oral drug delivery. *Nanotechnology*. 2011;22(27):1–12. doi:10.1088/0957-4484/22/27/275102

54. Calce E, Bugatti V, Vittoria V, De Luca S. Solvent-free synthesis of modified pectin compounds promoted by microwave irradiation. *Molecules*. 2012;17:12234–12242. doi:10.3390/molecules171012234

55. Kumar A, De A, Mozumdar S. Synthesis of acrylate guar-gum for delivery of bio-active molecules. *Bull Mater Sci*. 2015;38 (4):1025–1032. doi:10.1007/s12034-015-0930-z

56. Mofid V, Mousavi M, Djomeh ZE, Razavi SH, Gharibzahedi SMT, Jahanbakhsh F. Studying the interaction of xanthan gum and pectin with some functional carbohydrates on the rheological attributes of a low-fat spread. *J Disper Sci Technol*. 2014;35(8):1106–1113. doi:10.1080/01932691.2013.833479

57. Wamorkar V, Varma MM, Manjunath S. Formulation and evaluation of stomach specific in-situ gel of Metoclopramide using natural, bio-degradable polymers. *Int J Res Pharm Biomed Sci*. 2011;2 (1):193–201.

58. Kalanuria A, Peterlin B. A review of the pharmacokinetics, pharmacodynamics and efficacy of Zolmitriptan in the acute abortive treatment of migraine. *Clin Med Ther*. 2009;1:397–413.

59. Tao X, Li Y, Hu Q, et al. Preparation and drug release study of novel nanopharmaceuticals with polysorbate 80 surface adsorption. *J Nanomater*. 2018;2018:1–11. doi:10.1155/2018/4718045

60. Ishak RA, Mostafa NM, Kamel AO. Stealth lipid polymer hybrid nanoparticles loaded with rutin for effective brain delivery–comparative study with the gold standard (Tween 80): optimization, characterization and biodistribution. *Drug Deliv*. 2017;24(1):1874–1890. doi:10.1080/10717544.2017.1410263

61. Awadeen RH. *Formulation and Evaluation of in-situ Gelling Oral Sustained Release Dosage Forms for Certain Drugs [Dissertation]*. Egypt: University of Mansoura; 2018.